

Site-specific, genotypic and temporal variation in photosynthesis and its related biochemistry in wheat (*Triticum aestivum*)

Prabuddha Dehigaspitiya^A , Paul Milham^B, Anke Martin^A, Gavin Ash^A, Dananjali Gamage^C, Paul Holford^D and Saman Seneweera^{A,E,*} 

For full list of author affiliations and declarations see end of paper

***Correspondence to:**

Saman Seneweera
Centre for Crop Health, University of
Southern Queensland, Toowoomba,
Qld 4350, Australia
Email: Saman.Seneweera@usq.edu.au

Handling Editor:

Oula Ghannoum

Received: 13 April 2021

Accepted: 18 October 2021

Published: 14 December 2021

Cite this:

Dehigaspitiya P *et al.* (2022)
Functional Plant Biology, **49**(2), 115–131.
doi:[10.1071/FP21111](https://doi.org/10.1071/FP21111)

© 2022 The Author(s) (or their
employer(s)). Published by
CSIRO Publishing.

This is an open access article distributed
under the Creative Commons Attribution-
NonCommercial-NoDerivatives 4.0
International License (CC BY-NC-ND).

OPEN ACCESS

ABSTRACT

Photosynthesis in wheat (*Triticum aestivum* L.) pericarps may contribute appreciably to wheat grain yield. Consequently, we investigated the temporal variation of traits related to photosynthesis and sucrose metabolism in the pericarps and flag leaves of three wheat genotypes, Huandoy, Amurskaja 75 and Greece 25, which are reported to differ in expression of genes related to the C₄ pathway in wheat grain. Significant site-specific, genotypic and temporal variation in the maximum carboxylation rate ($V_{c_{max}}$) and maximum rates of electron transport (J_{max}) (biological capacity of carbon assimilation) were observed early in ontogeny that dissipated by late grain filling. Although the transcript abundance of *rbcS* and *rbcL* in flag leaves was significantly higher than in the pericarps, in line with their photosynthetic prominence, both organ types displayed similar expression patterns among growth stages. The higher N concentrations in the pericarps during grain enlargement suggest increased Rubisco; however, expression of *rbcS* and *rbcL* indicated the contrary. From heading to 14 days post-anthesis, wheat pericarps exhibited a strong, positive correlation between biological capacity for carbon assimilation and expression of key genes related to sucrose metabolism (*SPS1*, *SUS1* and *SPP1*). The strong correlation between spike dry weight and the biological capacity for carbon assimilation along with other findings of this study suggest that metabolic processes in wheat spikes may play a major role in grain filling, total yield and quality.

Keywords: biological capacity of carbon assimilation, grain filling, J_{max} , source and sink interaction, spike gas exchange, sucrose metabolism, transcript abundance, $V_{c_{max}}$.

Introduction

Significant yield improvement of critical C₃ cereal crops occurred between the 1950s and 1980s (Furbank *et al.* 2015) and has sustained global food demand for a number of decades. However, catering to the estimated global population of 9.8 billion by 2050 (Dillard 2019) necessitates a 60% yield improvement of critical food crops (White and Gardea-Torresdey 2018; Li *et al.* 2017). Reaching this target may not be possible without a further breakthrough, as the yield potential of most major cereal crops has plateaued (Furbank *et al.* 2015; Wang *et al.* 2017; Molero and Reynolds 2020).

Wheat (*Triticum aestivum* L.) is an important cereal crop for half the global population, and increasing the efficiency of photosynthesis is one possible solution to the upcoming food crisis (Jia *et al.* 2015; Kubis and Bar-Even 2019; van Bezouw *et al.* 2019; Molero and Reynolds 2020). However, inadequate understanding of the complex genetic processes of photosynthesis has held back improvement, because wheat is already photosynthetically efficient (Li *et al.* 2017). For instance, little is known about photosynthesis in wheat spikes (Jia *et al.* 2015; Zhang *et al.* 2020), which may contribute 10–40% of photosynthate to the filling grain (Serrago *et al.* 2013; Jia *et al.* 2015; Zhang *et al.* 2020), and photosynthesis in wheat spikes may also be as efficient as in leaves (Rangan *et al.* 2016; Molero and Reynolds 2020; Zhang *et al.* 2020).

Photosynthesis correlates strongly with plant sucrose metabolism (Vu *et al.* 2006; Vicente *et al.* 2015). When the sugar concentration of the photosynthetic tissue increases, genes in source tissues related to sucrose formation and amino acid synthesis are upregulated (Stitt *et al.* 2010; Paul and Pellny 2003) and sugars are translocated to sink tissues. This sink–source interaction is a determining factor in the grain yield of wheat (Rajala *et al.* 2009). The quantity of sugars produced from photosynthesis varies among different photosynthetic organs (Koch 2004; Molero and Reynolds 2020), which may lead to initiation of site-specific molecular level changes in sucrose metabolism. Therefore, knowledge of the expression patterns of key genes regulating sucrose metabolism in wheat pericarps during grain filling may illuminate the photosynthetic contribution by the spike to wheat grain yield and, consequently, deserves further exploration.

In the C₃ pathway under high irradiance, the amount of Rubisco is a determining factor for the rate of CO₂ assimilation throughout the life cycle of a photosynthetic organ (Suzuki *et al.* 2009). In higher plants, Rubisco consists of eight large subunits and eight small subunits. The small and the large subunits of Rubisco are coded from a multigene family, *rbcS*, in the nucleus, and a single gene, *rbcL*, in the chloroplast genome (Dean *et al.* 1989; Suzuki *et al.* 2009). The expression patterns of *rbcL* and *rbcS* mRNAs, and their activities, have been intensely studied in wheat leaves (Nie *et al.* 1995; Demirevska *et al.* 2009), whereas, less attention has been paid to the expression of *rbcL* and *rbcS* in wheat pericarps and spikes.

Exploration of the contribution of wheat spikes to grain filling requires assessment of the following features associated with photosynthesis: (1) gas exchange measurements of wheat spikes; (2) the expression patterns of the genes encoding the Rubisco precursors, *rbcL* and *rbcS* (Nie *et al.* 1995; Demirevska *et al.* 2009); and (3) the regulation of genes related to sucrose and amino acid synthesis (Paul and Pellny 2003; Stitt *et al.* 2010). All three types of observations are required because of the complex interactions between gas exchange, photosynthesis, sucrose metabolism and sink–source relationships (Vu *et al.* 2006; Vicente *et al.* 2015). Additionally, total nitrogen (N) in leaves is a simple yet useful measure of C assimilation and protein synthesis, because Rubisco accounts for 15–30% of their total N (Makino *et al.* 1992; Suzuki *et al.* 2009; Seneweera *et al.* 2011), and Rubisco degradation products are a source of N for developing tissues such as the grain (Suzuki *et al.* 2001; Makino *et al.* 1984).

The main hypotheses of this study are that: (1) C assimilation varies genotypically and temporally between the flag leaves and spikes of wheat; and (2) spike photosynthesis may overtake leaves at late grain filling. These hypotheses were tested using three winter wheat varieties Huandoy, Amurskaja 75 and Greece 25 that had previously been reported to express

genes related to C₄ pathway in their grains/spikes (Rangan *et al.* 2016).

Materials and methods

Plant materials and growth conditions

Three winter wheat (*Triticum aestivum* L.: Poales, Poaceae) varieties Amurskaja 75, Greece 25 and Huandoy were selected based on previously reported differences in the expression of genes related to C₄ pathway in the pericarps (Rangan *et al.* 2016). Seeds were sourced from the Australian Grain Gene Bank, Horsham, Australia. Five seeds were sown in each pot containing 4.2 kg of loam soil and 14 day after sowing the number of seedlings was reduced to two per pot. There were 12 replicate pots per treatment. Soil water was maintained at field capacity by daily watering.

The study was conducted in a greenhouse in Queensland, Australia (27°33′38.02″S, 151°55′55.20″E) from May to October (winter) and the maximum/minimum temperatures were 22/14°C. The midday light intensity of the greenhouse was 1000–1500 PAR and the RH of the air was 50–70%. The experimental design was completely randomised with 12 replicates. Pot positions were rerandomised weekly to minimise any location effects inside the greenhouse.

Morphological measurements

Three replicates from four growth stages [heading, 14 days post-anthesis (14 dpa), 30 dpa and maturity (CM)] were used for phenotyping. The traits measured and growth stages of data collection are shown in Supplementary Table S1. Leaf area was measured using the Li-COR leaf area meter (LI-COR, USA) and spike area was calculated using the following equation:

$$A \approx 2\pi L \sqrt{\frac{(a/2)^2 + (b/2)^2}{2}}$$

Each spike was considered as an elliptical cylinder (Supplementary Fig. S1). ‘A’ is the surface area (assumed photosynthetic area) of the wheat spike, *a* and *b* denote the diameters of the short and long axis of the ellipse, respectively (Fig. S1), *L* is the length of the spike/cylinder. Five values of *a* and *b* were measured and averaged.

The harvest index (HI) was calculated as: (weight of the total harvest)/(above ground biomass); and by analogy, the spike area index (SAI) was calculated as: (spike area)/(total photosynthetic area). After leaf and spike area measurements, samples were dried at 60°C for 72 h and weighed.

Gas exchange

Gas exchange parameters of the flag leaves and wheat spikes were assessed on four occasions: (1) at heading;

(2) 3 dpa; (3) 14 dpa; and (4) 30 dpa. Plants were introduced into a controlled growth chamber (PGC-105, Percival, USA) at least 1 h prior to the measurements where the temperature, canopy light intensity and relative humidity were maintained at 22°C, 1000 $\mu\text{mol m}^{-2} \text{s}^{-1}$ and 70%, respectively.

The measurements on flag leaves and spikes were carried out between 09 00 hours and 14 30 hours using a portable photosynthesis system (LI-6400xt, LI-COR) (Evans and Santiago 2014). For spikes, the LI-6400xt was coupled with a transparent conifer chamber (6400-05, LI-COR). Spike level temperature and the air flow rate were maintained at 22°C and 500 $\mu\text{mol s}^{-1}$, respectively. Photosynthetically active radiation (PAR) of the controlled growth chamber was maintained as 1000 $\mu\text{mol m}^{-2} \text{s}^{-1}$. Steady state gas exchange was reached in about 10–15 min. The initial reference CO_2 concentration inside the conifer chamber was 400 $\mu\text{mol mol}^{-1}$, and the relative humidity was maintained at 50–70%. Each spike was equilibrated for a few minutes until gas exchange reached steady state before measurements commenced.

Photosynthesis (A), stomatal conductance (g_s), intercellular CO_2 concentration (C_i) and the ratio between C_i and ambient CO_2 concentration (C_a) (C_i/C_a) and carbon dioxide response ($A-C_i$) curves were obtained for flag leaves and wheat spikes at each growth stage. After taking measurements under light, the light source of the growth cabinet was turned off and the plants were allowed to stabilise for 45 min before measuring gas exchange of wheat spikes in the dark (R_D). Spike photosynthesis (A_s) was obtained by subtracting R_D from A_R , where P_R is the rate of photosynthesis under PAR (Molero and Reynolds 2020). The biological capacity of carbon assimilation for both wheat spikes and flag leaves ($V_{c_{\max}}$ and J_{\max}) in different growth stages were calculated using the fitted models based on the $A-C_i$ curves.

Measurements of plant carbon and nitrogen

Oven-dried pericarps and flag leaves of three genotypes at the four growth stages were removed from the plants and ground in a ball mill (Tissue Lyser II, QIAGEN, Australia) to $\sim 100 \mu\text{m}$ diameter. Carbon and nitrogen (C and N) contents of the plant samples were measured using a combustion analyser (Leco CN628, USA).

Gene expression

At least nine enzymes are involved in sucrose metabolism, including sucrose synthase (SUS), sucrose phosphate phosphatase (SPP) and sucrose phosphate synthase (SPS) (Jia *et al.* 2015). We focused on the mRNA abundance of these three enzymes since they may have major roles in sucrose biosynthesis. The transcript abundance of key genes associated with photosynthesis was also assessed.

Sample collection, RNA extraction, quantification and cDNA synthesis

Three replicates of wheat spikes and flag leaves from the main tiller at heading were harvested 14 and 30 dpa between 11 00 hours and 13 00 hours using chilled blades, placed in chilled storage tubes and immediately submerged in liquid N_2 . Samples were subsequently stored at -80°C until total RNA extraction. Decontaminated and RNase free mortars and pestles were stored at -80°C , in a sealed polythene bag, at least 12 h prior to the extraction. TPS buffer was prepared using 10 mM EDTA, 1 M KCl, and 100 mM Tris-HCl. After adjusting the pH to 8, the buffer was autoclaved and cooled to room temperature. Mortars and pestles were chilled using liquid N_2 before ~ 200 mg of the outermost layer of the wheat pericarp and flag leaves were dissected and placed into separate chilled mortars. Plant samples were ground to a fine powder in liquid N_2 . Five hundred μL of Trizol reagent (Invitrogen, Thermo Fisher Scientific, USA) and 700 μL of TPS buffer were added to the ground plant samples and the grinding was continued. The homogenised solutions were collected in 2.5 mL RNase-free, autoclaved microcentrifuge tubes and incubated at room temperature for 10 min. A total of 120 μL of chloroform (per 200 mg of plant tissue) was added to the incubated samples and mixed gently. The samples were incubated for another 3 min before being centrifuged for 15 min at 26 319g at 4°C (Eppendorf centrifuge 5424R, Australia). After phase separation, the supernatant was collected in a new set of RNase-free microcentrifuge tubes and 600 μL of ice-cold isopropanol was added (biotechnology grade, Sigma-Aldrich, USA). The sample tubes were gently mixed and incubated for 10 min. To separate the precipitated RNA, tubes were centrifuged for 10 min at 26 319g at 4°C. After removing the supernatant, 600 μL of 75% ethyl alcohol (Biotechnology grade, Sigma-Aldrich, USA) was added to each tube. To purify RNA pellets, tubes were centrifuged for 5 min at 26 319g at 4°C. After removing ethyl alcohol, samples were air dried, 30 μL of diethylpyrocarbonate (DEPC) treated water (Sigma-Aldrich) was added to each tube to dissolve the RNA and the samples were stored at -80°C until further use.

RNA was quantified using a Qubit fluorimeter (Invitrogen by Thermo Fisher Scientific) according to the manufacturer's instructions. Concentrations of the RNA samples were adjusted to 1 $\mu\text{g } \mu\text{L}^{-1}$. RNA samples were treated with amplification grade DNase I (Invitrogen by Thermo Fisher Scientific) according to the manufacturer's instructions. RNA samples were reverse-transcribed using a SensiFAST cDNA synthesis kit (Catalogue No – Bio-65054, Bioline, UK) as per the manufacturer's instructions, and the samples (20 μL reaction volume) were introduced into the thermal cycler set at 25°C for 10 min for primer annealing, 42°C for 15 min for reverse transcription and 85°C for 5 min for inactivation.

Primer selection and quantitative reverse transcription polymerase chain reaction (qRT-PCR)

The primer sequences of the genes associated with photosynthesis and sucrose metabolism (Table S5) were taken from Vicente *et al.* (2015) and Bachir *et al.* (2017). The specificity of the primers for *T. aestivum* was tested using the Primer-Blast option in the National Centre for Biotechnology Information (NCBI) website (<https://www.ncbi.nlm.nih.gov>). Primers were sourced from Integrated DNA Technologies, Inc. (Integrated DNA Technologies Pty. Ltd, Republic of Singapore).

Reactions were carried out in 96-well plates using a QuantStudio 3 real-time PCR system (Applied Biosystems, Thermo Fisher Scientific, USA). Each reaction mixture contained 4 μ L of cDNA, 4 μ L of DEPC treated water, 10 μ L of PowerUp SYBR Green Master (Applied Biosystems from Thermo Fisher Scientific, USA), 1 μ L of 10 mM forward primer and 1 μ L of 10 mM reverse primer. Three biological replicates were used for each growing stage of the three wheat genotypes. The PCR program was set at 95°C for 10 min followed by 40 cycles of 95°C for 15 s and 60°C for 1 min.

Statistical analysis

Before statistical analysis, any data that were not normally distributed were transformed for normality. To determine the significance of different growth stages, organ types and genotypes, ANOVA was performed. Tukey's tests and standard errors of differences were used to determine the differences between growth stages, organ types and genotypes at $P < 0.05$ significant level. Pearson product-moment correlations were used to test potential correlations between harvest related traits and parameters associated with biological capacity of C assimilation and with gene expression related to sucrose metabolism. Data analysis was conducted using SPSS statistical software ver. 23 (IBM, Armonk, NY, USA). GraphPad Prism scientific software ver. 8 (GraphPad Software, San Diego, CA) was used for graphical representation of the data. Primer efficiencies of the reactions of gene expression analysis were determined using the LinRegPCR software ver. 2012. Relative gene expression of three varieties of two organ types at different growth stages was calculated using the comparative threshold cycle (C_t) $2^{-\Delta\Delta C_t}$ method.

Results

Growth-related traits

There were statistically significant effects of genotype and growth stage on growth-related traits including total spike weight ($P < 0.001$), total aboveground biomass (TAB) ($P < 0.001$), plant height ($P < 0.01$), biomass without spikes (BWS) ($P < 0.001$) and total biomass (TB) ($P < 0.001$) (Fig. 1a–e). Highest spike weight was shown in the variety Huandoy and the highest aboveground biomass was reported

in Amurskaja 75 (Figs 1a–e). Results indicated that the total biomass without spikes increased from heading to 14 dpa across all three genotypes and showed a clear decline after 14 dpa.

Photosynthesis-related traits

Genotype and growth stage had statistically significant interactions on the photosynthetic areas of total spikes (PAS) ($P < 0.01$), the spikes of the main tillers (PASM) ($P < 0.01$), and leaves (PAL) ($P < 0.01$), as well as total photosynthetic area (PAT) ($P < 0.01$), spike area index (SAI) ($P < 0.001$) and the ratio between total spike area and total leaf area (PAS/PAL) ($P < 0.001$) (Fig. 2a–f). From all three genotypes, Huandoy showed the highest total spike photosynthesis across all three growth stages considered in the study. Amurskaja 75 showed the highest photosynthetic area of the flag leaves of the three genotypes (Fig. 2a–f); highest photosynthetic area of leaves and total photosynthetic area including spikes (Fig. 2b). In addition, highest spike area index and PAS/PAL ratios were reported in Huandoy (Fig. 2f).

Harvest-related traits

Genotype affected tiller number ($P < 0.01$), total harvest (TH) ($P < 0.001$) and harvest index (HI) ($P < 0.001$) but not spike number (Fig. 3). Total harvest and HI were higher in Huandoy than other genotypes, while Amurskaja 75 had the highest number of spikes and tillers at maturity.

Gas exchange differences between genotypes and during ontogeny

In Huandoy, the highest A was observed at 14 dpa for both spikes and flag leaves (Fig. 4) while in Greece 25, the highest A was exhibited at heading. In general, at the early reproductive stages (heading to 14 dpa), the A was significantly higher in flag leaves than in wheat spikes (Fig. 4). However, at 30 dpa, a reduction in A was observed between spikes and flag leaves of all genotypes. Interestingly, at 30 dpa, the A of wheat spikes was much higher than the flag leaf photosynthesis for both Huandoy and Greece 25. Further, in all the instances, the C_i/C_a was between 0.626 and 0.81 (Fig. 4). Overall, there were significant interactions among genotypes, growth stages and organ types for $V_{c_{max}}$, J_{max} , and trios phosphate utilisation (TPU) (Table S2, S3 and S4). However, the effect of genotype itself for $V_{c_{max}}$ of flag leaves was not statistically significant (Table S2, S3 and S4). All the genotypes displayed their highest and the lowest $V_{c_{max}}$, J_{max} and TPU for both spikes and flag leaves at early to mid-grain reproductive stages (heading to 14 dpa) and 30 dpa, respectively (Figs 5 and 6). The $V_{c_{max}}$ of wheat spikes displayed higher variation between growth stages than the $V_{c_{max}}$ of flag leaves (Figs 5a–c and 6a–c).

The $V_{c_{max}}$, J_{max} , and TPU of flag leaves were significantly higher than in spikes at early reproductive stages (heading to

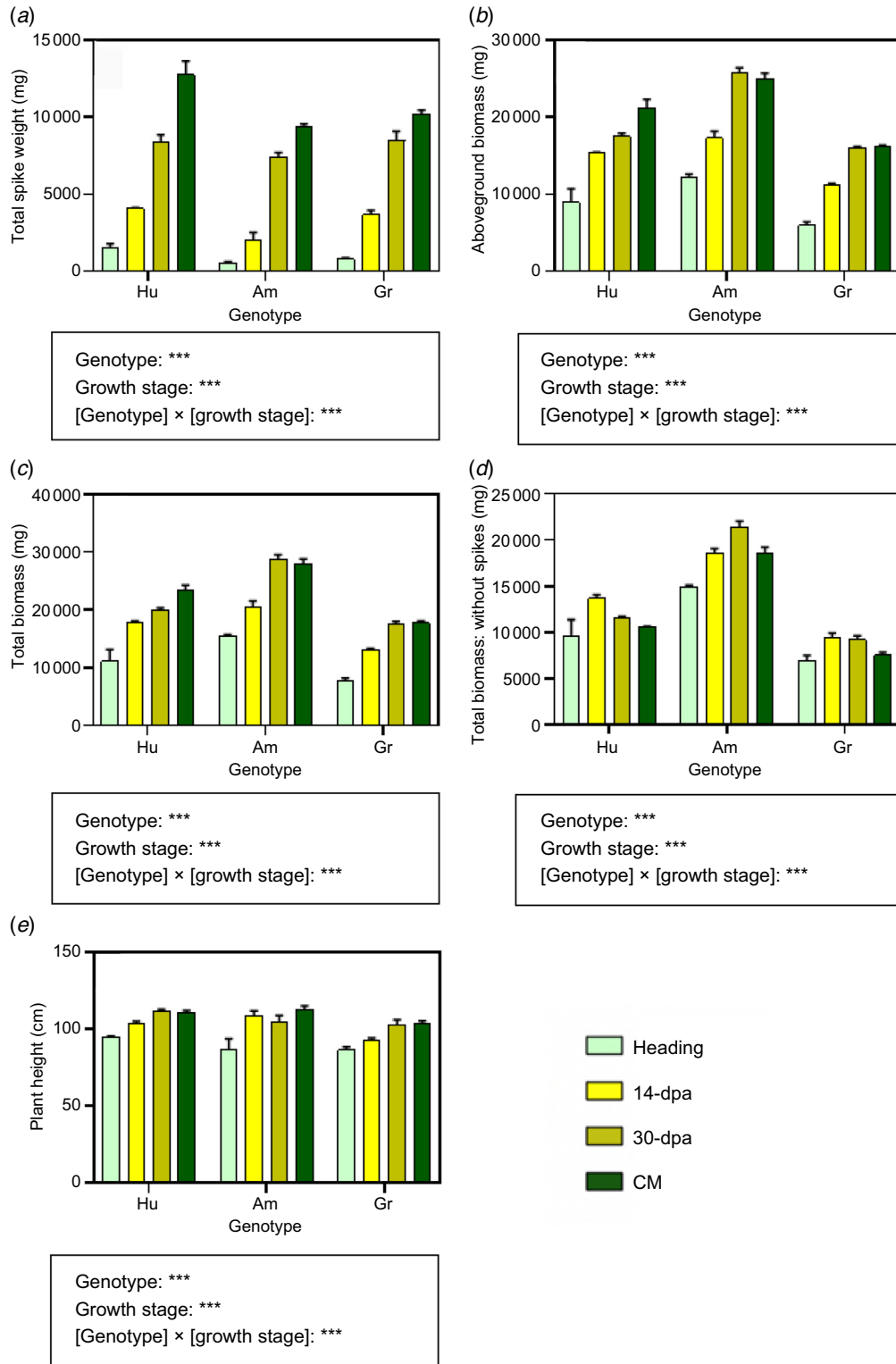


Fig. 1. Variation in growth-related traits. (a) Total spike weight, (b) total above ground biomass (AGB), (c) total biomass (TB), (d) total biomass without spikes (BWS) and (e) plant height between three genotypes in four different growth stages. $n = 3$. Hu, Huandoy; Am, Amurskaja 75; Gr, Greece 25; CM, maturity; ** $p < 0.01$; *** $p < 0.001$.

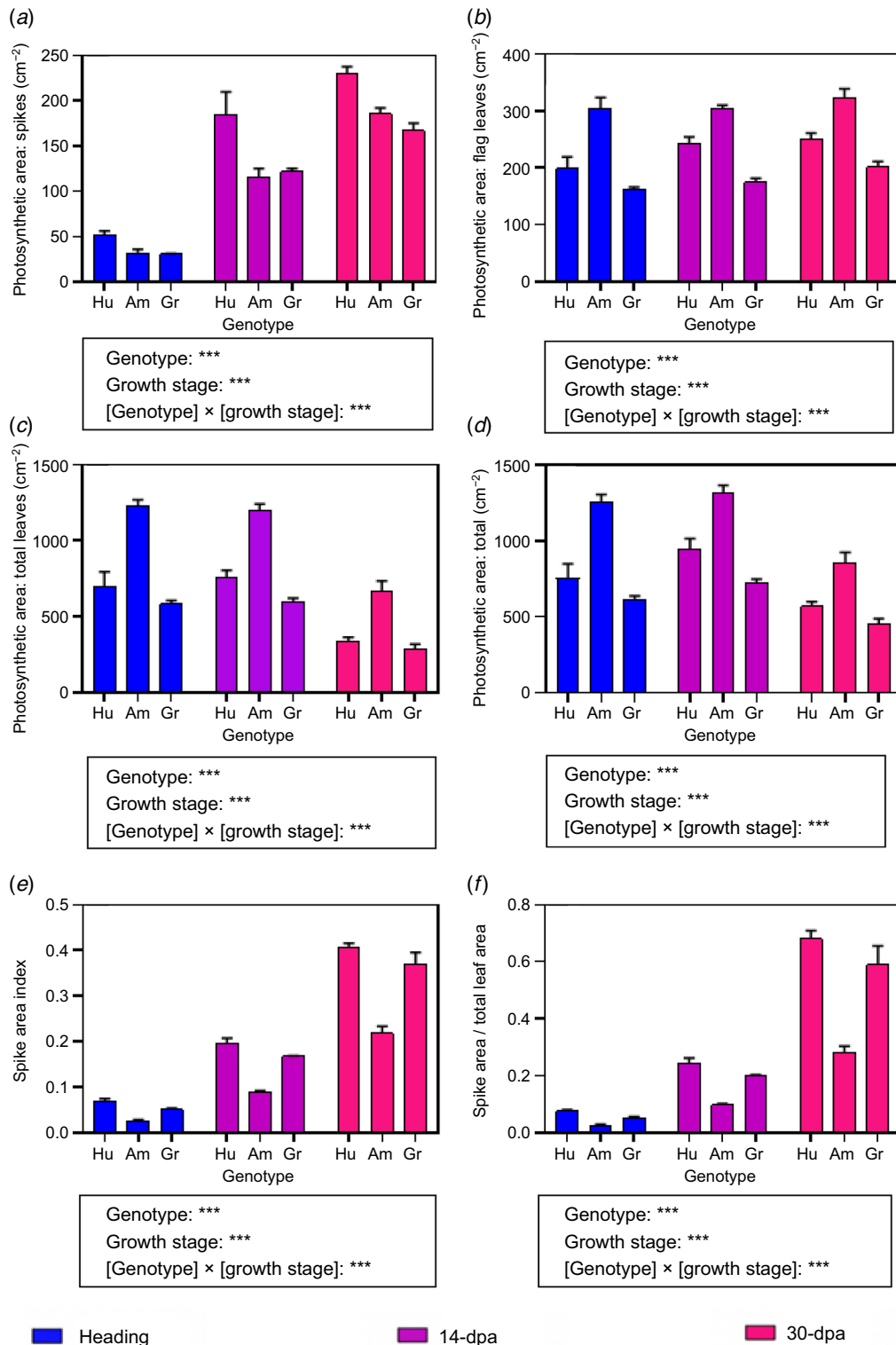


Fig. 2. Variation of (a) photosynthetic area of spikes, (b) photosynthetic area of flag leaves, (c) photosynthetic area of total leaves, (d) total photosynthetic area, (e) spike area index and (f) spike area/total leaf area between considered wheat genotypes at three growth stages. *n* = 3. Hu, Huandoy; Am, Amurskaja 75; Gr, Greece 25; ***P* < 0.01; ****P* < 0.001.

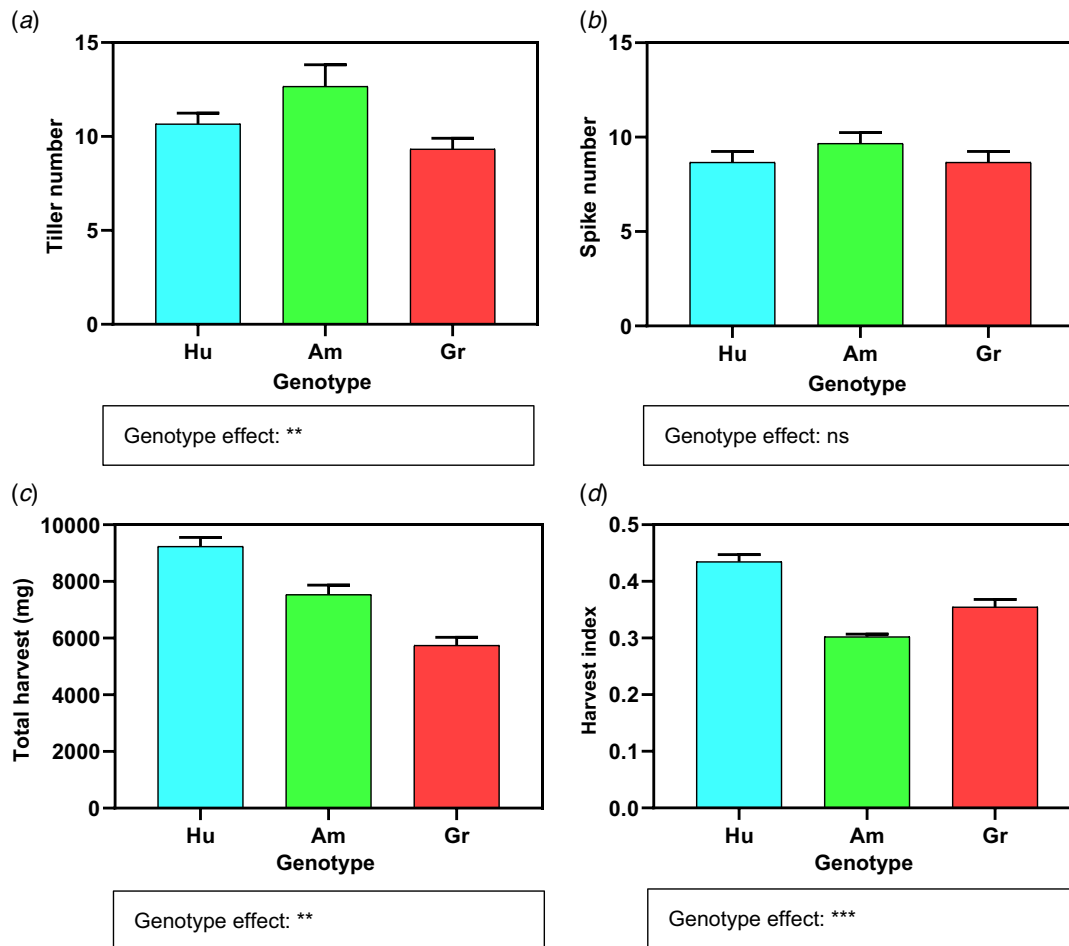


Fig. 3. Variation in (a) tiller number, (b) spike number, (c) total harvest and (d) harvest index between three wheat genotypes at maturity (CM). $n = 3$. Hu, Huandoy; Am, Amurskaja 75; Gr, Greece 25; ** $P < 0.01$; *** $P < 0.001$; n.s., not significant.

14 dpa) (Figs 5 and 6). Interestingly, during late-grain filling (30 dpa), the C assimilation capacity of spikes and flag leaves was not statistically different ($P > 0.05$, Table 1) (Fig. 7).

Site-specific, genotypic and temporal variation of N concentrations

From heading to 14 dpa, N concentration increased in the pericarps and was unchanged in flag leaves (Fig. 8). Overall, N concentrations of flag leaves were appreciably higher than in the pericarps. In pericarps and flag leaves, there was a significant interaction between genotype and growth stage on N concentrations ($P < 0.001$), with the lowest N concentrations occurring at maturity (Fig. 8). Greece 25 had the greatest N concentration in both pericarps and flag leaves at all four growth stages (Fig. 8).

Expression of genes associated with photosynthesis

The 3 dpa stage was omitted from gene expression analysis since differences in $V_{c,max}$, J_{max} and TPU between heading and

3 dpa were typically minimal. With respect to the expression of *rbcS*, a significant three-way interactions occurred between genotype, organ type and growth stage ($P < 0.001$) (Table 2). However, there were no statistically significant interactions in *rbcL* expression between genotype and organ type ($P > 0.05$), and genotype, organ type and growth stage (Table 2).

In all genotypes, the expression of *rbcL* and *rbcS* displayed a decrease in both pericarps and flag leaves towards 30 dpa. Of the two genes, the relative expression of *rbcL* was significantly higher than *rbcS* at all growth stages. Also, the relative expression of both *rbcL* and *rbcS* were significantly greater in flag leaves than in pericarps. The genotype Greece displayed the highest relative expression for *rbcS* in both pericarps and flag leaves (Table 3). In pericarps, the mean relative expression of *rbcL* at heading was 83-, 37- and 20-fold greater than the expression of *rbcS* in Huandoy, Amurskaja 75 and Greece 25, respectively (Table 3). Further, in pericarps at heading, Amurskaja 75 and Greece 25 had the highest and the lowest relative expressions for *rbcL*, respectively (Table 3).

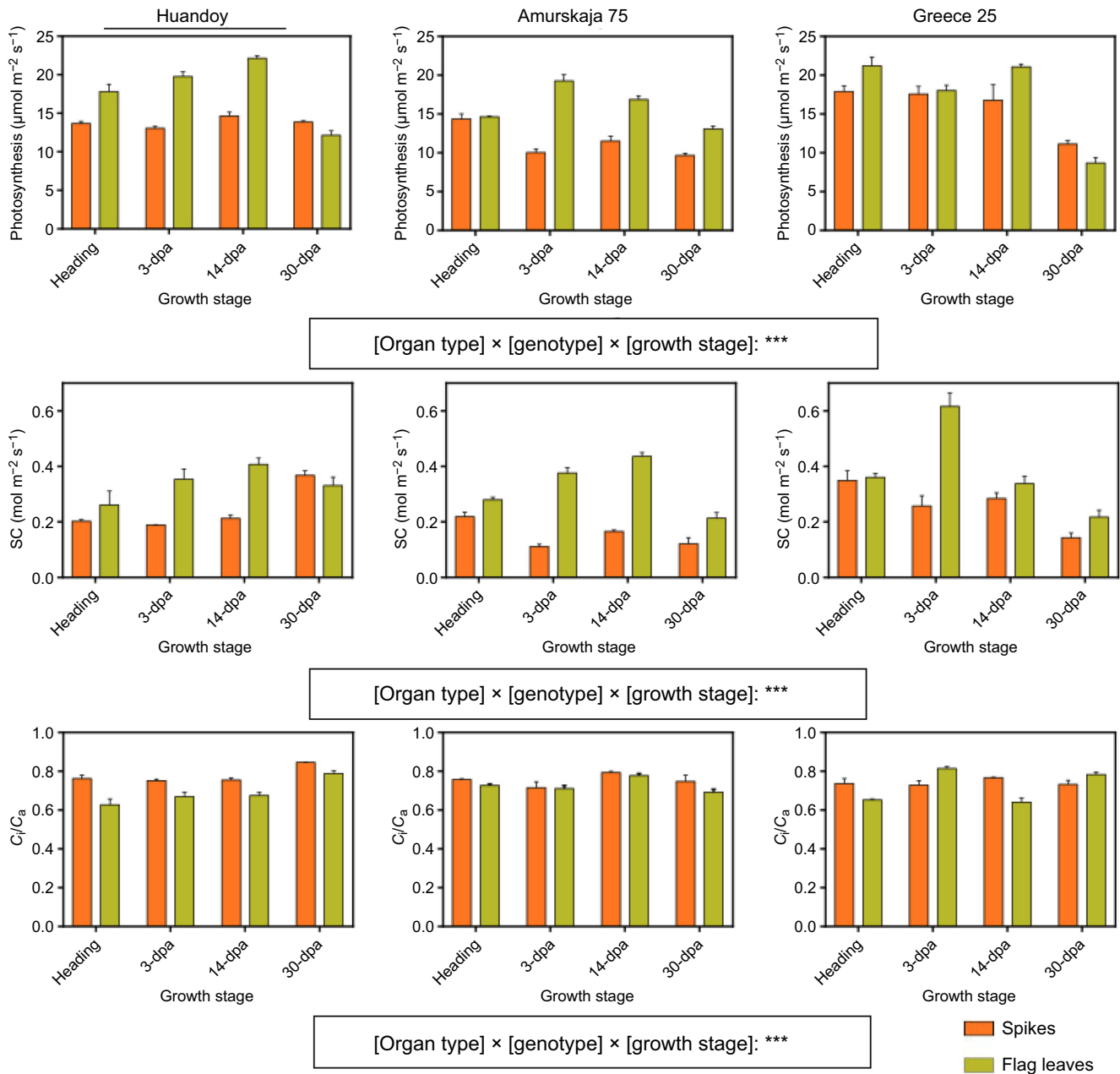


Fig. 4. Variation of photosynthesis (A), stomatal conductance (SC) and the ratio between intercellular to ambient CO₂ concentrations (C_i/C_a) between wheat pericarps and flag leaves of three wheat genotypes at different growth stages. Hu, Huandoy; Am, Amurskaja 75; Gr, Greece 25; ***P < 0.001.

Expression of key genes related to sucrose metabolism

A significant three-way interaction occurred between genotype, organ type and growth stage on the expression of *SPS1* (P < 0.001) (Table 2). Likewise, genotype and organ type, and genotype and growth stage had significant interactions on expression of *SUS1* and *SPP1* (Table 2). However, organ type and growth stage did not interact with *SPP1* expression (Table 2).

In pericarps, expression of *SPS1* and *SUS1* increased with growth stage for Huandoy, while for Amurskaja 75 and Greece 25 the trend was to decrease (Table 3). Generally, the expression of these genes was higher in the early and mid-reproductive stages (heading and 14 dpa) than during late-grain filling (30 dpa).

In flag leaves, there was considerable variation in the expression of *SPS1*, *SUS1* and *SPP1* among the three growth stages. Further, as for flag leaves, expression of *SPS1* and *SUS1*

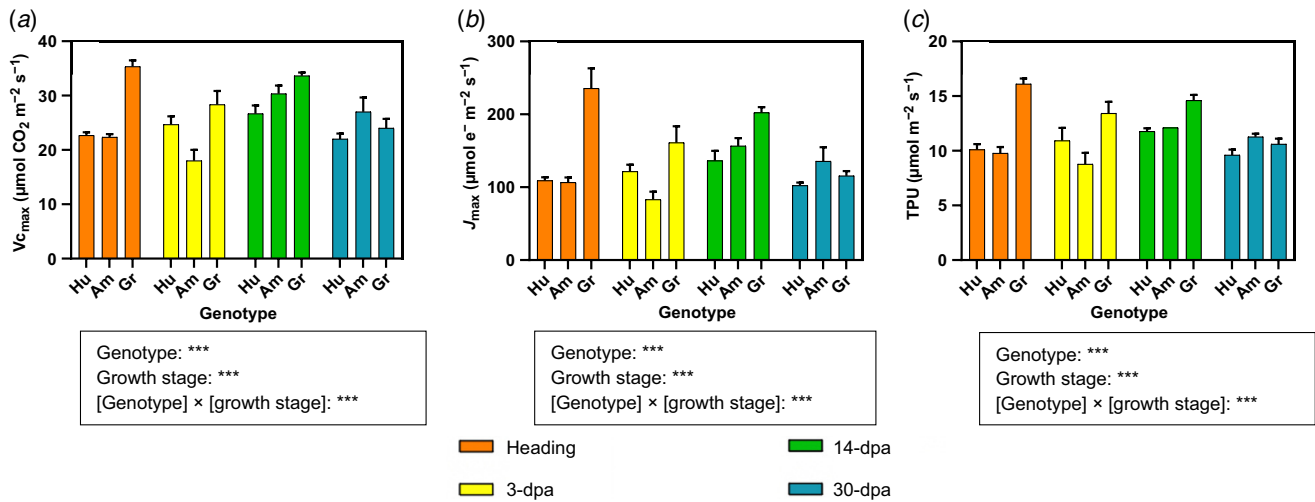


Fig. 5. Changes in (a) $V_{c_{max}}$, (b) J_{max} and (c) TPU of three wheat genotypes at four growth stages in wheat spikes. $n = 3$. Hu, Huandoy; Am, Amurskaja 75; Gr, Greece 25; *** $P < 0.001$.

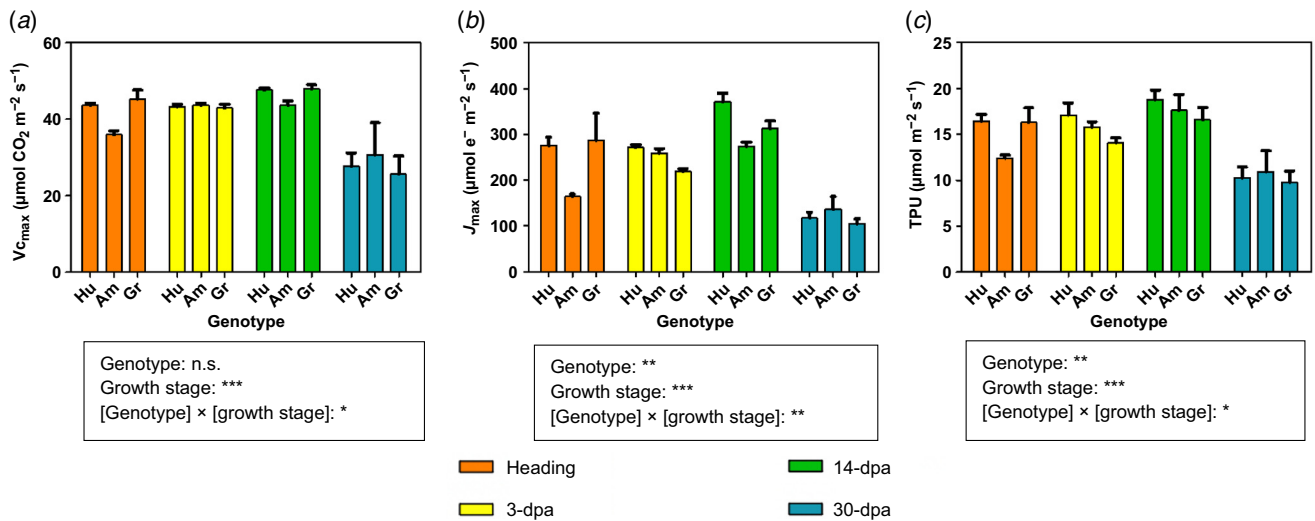


Fig. 6. Changes in (a) $V_{c_{max}}$, (b) J_{max} and (c) TPU of three wheat genotypes at four growth stages in flag leaves of wheat. $n = 3$. Hu, Huandoy; Am, Amurskaja 75; Gr, Greece 25; * $P < 0.05$; ** $P < 0.01$; *** $P < 0.001$; n.s., not significant.

in Huandoy increased over time, while in Amurskaja 75 and Greece 25 the trend was for *SPS1* expression to decrease.

When comparing the two organ types, both pericarps and flag leaves of Huandoy and Amurskaja 75 had similar expression patterns for *SPS1*, *SUS1* and *SPP1* (Table 3). Generally, the expression of *SPS1* and *SUS1* was much higher in flag leaves than in pericarps (Table 3). In contrast, the expression of *SPP1* was much higher in pericarps than in flag leaves of Amurskaja 75 and Greece 25.

Spike dry weights and the biological capacity for carbon assimilation

To obtain a holistic idea about the plant photosynthetic parameters, values of $V_{c_{max}}$, J_{max} and TPU of spikes at

different growth stages were multiplied by the total spike area at each growth stage. Strong, positive correlations between spike dry weight and [$V_{c_{max}}$] × [spike area] ($r = 0.800$, $P < 0.01$), spike dry weight and [J_{max}] × [spike area] ($r = 0.720$, $P < 0.01$), and, spike dry weight and [TPU] × [spike area] ($r = 0.813$, $P < 0.01$) were observed.

The biological capacity of carbon assimilation and the expression of genes of sucrose metabolism at early reproductive stages

At heading in spikes of all three genotypes, strong, positive correlations were observed between $V_{c_{max}}$ and the expression of *SUS1* ($r = 0.816$, $P < 0.01$), $V_{c_{max}}$ and the expression of *SPP1* ($r = 0.946$, $P < 0.01$), J_{max} and the expression of *SUS1*

Table 1. Comparison of $V_{c_{max}}$, J_{max} and TPU between wheat spikes and flag leaves of three genotypes at four growth stages.

Growth stage	Trait	Huandoy			Amurskaja 75			Greece 25		
		Mean values		Significance	Mean values		Significance	Mean values		Significance
		Spike	Flag leaf		Spike	Flag leaf		Spike	Flag leaf	
Heading	$V_{c_{max}}$	22.67	43.67	***	22.30	36.00	***	35.33	45.33	**
	J_{max}	109.00	275.67	***	106.67	164.00	***	235.67	287.33	n.s.
	TPU	10.10	16.43	***	9.77	15.77	**	16.10	16.27	n.s.
3 dpa	$V_{c_{max}}$	24.67	43.33	***	18.00	43.67	***	28.33	43.00	**
	J_{max}	121.67	271.33	***	83.00	259.00	***	161.00	218.67	*
	TPU	10.93	17.10	**	8.77	15.77	**	13.43	14.10	n.s.
14 dpa	$V_{c_{max}}$	26.67	47.67	***	30.33	43.67	**	33.67	48.00	**
	J_{max}	136.33	370.00	***	156.67	273.67	**	202.33	312.67	**
	TPU	11.77	18.77	***	12.10	17.60	**	14.60	16.60	n.s.
30 dpa	$V_{c_{max}}$	22.00	27.67	n.s.	27.00	30.67	n.s.	24.00	25.67	n.s.
	J_{max}	102.33	117.33	n.s.	135.67	136.33	n.s.	115.67	105.33	n.s.
	TPU	9.60	10.27	n.s.	11.27	10.93	n.s.	10.60	9.77	n.s.

Note: Summary of multivariate analysis is shown.

* $P < 0.05$; ** $P < 0.01$; *** $P < 0.001$.

dpa, days post anthesis; n.s., not significant.

($r = 0.851$, $P < 0.01$), J_{max} and the expression of *SPP1* ($R = 0.959$, $P < 0.01$), TPU and the expression of *SUS1* ($r = 0.799$, $P < 0.01$), and, TPU and the expression of *SPP1* ($r = 0.932$, $P < 0.01$). At 14-dpa, strong positive correlations were observed between $V_{c_{max}}$ and the expression of *SPS1* ($r = 0.786$, $P < 0.05$), $V_{c_{max}}$ and the expression of *SPP1* ($r = 0.817$, $P < 0.01$), J_{max} and the expression of *SPS1* ($r = 0.769$, $P < 0.05$), J_{max} and the expression of *SPP1* ($r = 0.7909$, $P < 0.05$), TPU and the expression of *SPS1* ($r = 0.807$, $P < 0.01$), and, TPU and the expression of *SPP1* ($r = 0.795$, $P < 0.05$). However, at later growth stages (30 dpa) in pericarps, this strong correlations between spike photosynthetic parameters and gene expression of sucrose metabolism could not be observed. Likewise, in flag leaves, positive correlations were not observed between photosynthetic parameters and gene expression of sucrose metabolism.

Discussion

Temporal trends in biomass accumulation of wheat spikes

Grain development consists of two overlapping stages: (1) grain enlargement, and (2) grain filling. The first commences at fertilisation and is a period of mitotic activity during which the potential to accumulate biomass is established; a substrate effect influences this potential. Wheat endosperm starts accumulating dry matter during the grain enlargement phase; i.e. at 15–20 dpa and continues until the spike reaches

maturity (35–40 dpa). Genetic, morphological and environmental factors play important roles in determining the rate and the duration of this second stage (Jenner *et al.* 1991). In this study, for all three genotypes, the fastest rate of biomass accumulation by spikes was between 14 dpa and 30 dpa. Moreover, during the same period, in most occasions, biomass without spikes decreased while total biomass increased. This means that most of the photosynthetic products from the grain enlargement phase to maturity accumulated in wheat spikes especially in the wheat grain.

In general, our results reveal that the biological capacity for C assimilation of wheat spikes (as assessed by $V_{c_{max}}$ and J_{max}) was greatest at 14 dpa, supporting the possibility that the spikes may make a prominent contribution to starch biosynthesis and accumulation in the grain (Fig. S2). However, to obtain a complete idea, the remobilisation of photosynthetic products to spikes from other photosynthetic organs such as leaves also has to be considered. A strong correlation between $V_{c_{max}}$ and the tissue N content was reported by Walker *et al.* (2014). Consistent with this proposition, in the present study, the highest N concentrations in wheat pericarps was at 14 dpa, the phase that displayed the highest $V_{c_{max}}$ and J_{max} . Rubisco is the key enzyme of C assimilation and plays a central role in C_3 photosynthesis (Suzuki *et al.* 2001), comprising a significant proportion of the N content of photosynthetic organs. Consequently, it is not unreasonable to assume that peaking of the N content in wheat pericarps during grain enlargement reflects peaking of Rubisco.

The remobilisation of N from the vegetative organs of the wheat plant to the grain takes place during mid to late grain

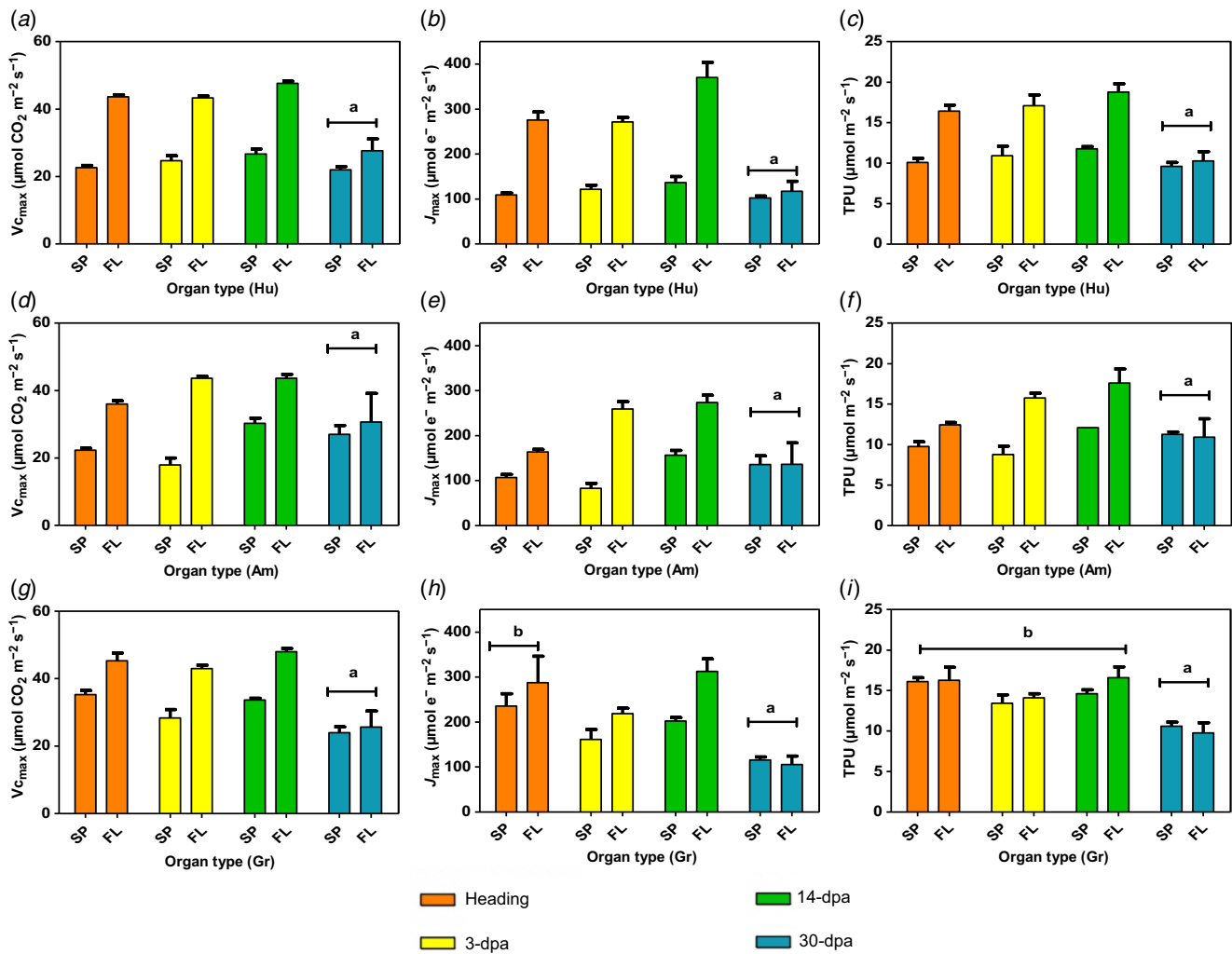


Fig. 7. Comparison between wheat spikes and flag leaves of (a) Huandoy: $V_{c_{max}}$, (b) Huandoy: J_{max} (c) Huandoy TPU (d) Amurskaja 75: $V_{c_{max}}$ (e) Amurskaja 75: J_{max} (f) Amurskaja 75: TPU (g) Greece 25: $V_{c_{max}}$ (h) Greece 25: J_{max} and (i) Greece 25: TPU. $n = 3$. Brackets with lowercase 'a and b' represents statistically not significant. Hu, Huandoy; Am, Amurskaja 75; Gr, Greece 25; SP, wheat spikes; FL, wheat flag leaves.

filling, and depends on genotypic and environmental factors (Barbottin *et al.* 2005). In this study, the low N concentrations in flag leaves at late grain filling (30 dpa) are consistent with remobilisation. From the current study, considerable variation in organ-specific N concentrations among genotypes was recorded. However, the variation in N concentrations in wheat flag leaves was not as significant as in the wheat pericarps (Fig. S2) indicating organ specific variation in N metabolism.

Lastly, there is a considerable genotypic variation in growth and harvest-related factors including: total spike weight, AGB, TB, BWS, HI and TH, as expected from previous research (Darroch and Baker 1990). It has also been reported that the duration of grain filling determines the time to maturity and the yield (Darroch and Baker 1990).

Temporal trends in transcript abundance of *rbcl* and *rbcs* between organ types

Transcript abundance of *rbcl* and *rbcs* in this study revealed site-specific and temporal variation in Rubisco metabolism in the wheat genotypes. Pericarps of Greece 25 and Amurskaja 75 displayed the highest *rbcs* and *rbcl* expression, respectively, at heading. Likewise, in flag leaves at heading, Greece 25 displayed the highest abundance of *rbcs*. *rbcl* and *rbcs* encode the two subunits of Rubisco, the enzyme that limits light-saturated C assimilation under current atmospheric conditions and is important in both C and N metabolism of plants (Suzuki *et al.* 2009; Jia *et al.* 2015). In grasses, Rubisco contents increase during leaf growth, peak at full expansion, then decline during senescence (Suzuki *et al.* 2010). However, our results did not show a similar

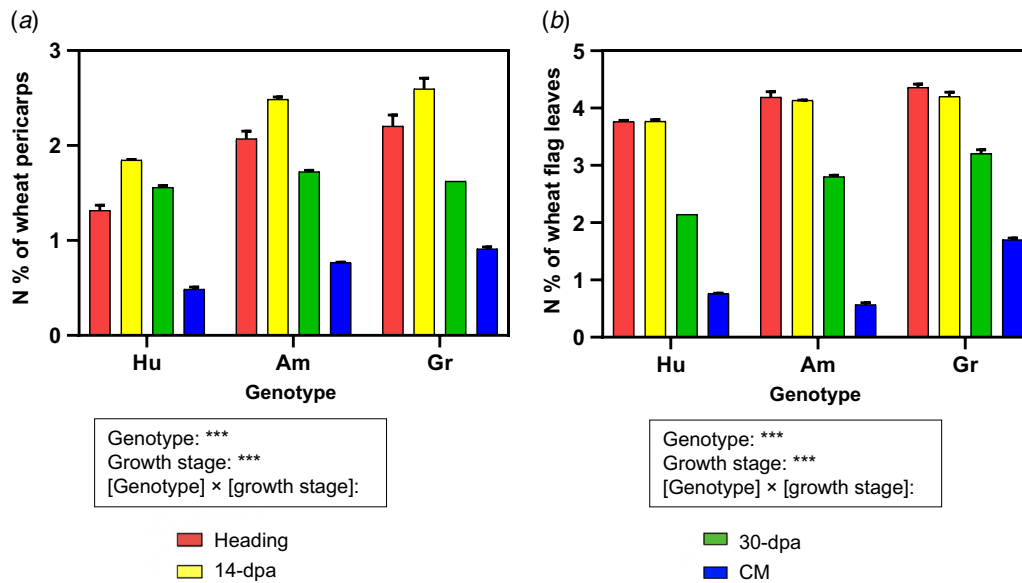


Fig. 8. Changes in (a) nitrogen percentages in wheat pericarps, and (b) nitrogen concentrations in wheat flag leaves of three wheat genotypes at four growth stages. $n = 3$. Hu, Huandoy; Am, Amurskaja 75; Gr, Greece 25; *** $p < 0.001$.

Table 2. The effect of genotype, organ type, growth stage and their interactions for *rbcL*, *rbcS*, *SPS1*, *SUS1*, and *SPP1* expression in wheat pericarps and flag leaves.

Metabolism	Gene	Individual effect			Interaction effect			
		Genotype effect	Organ type effect	Growth stage effect	Genotype × organ type	Genotype × growth stage	Organ type × growth stage	Genotype × organ type × growth stage
Photosynthesis	<i>rbcL</i>	*	***	***	n.s.	**	***	n.s.
	<i>rbcS</i>	*	***	***	*	***	***	***
Carbon metabolism	<i>SPS1</i>	*	***	**	***	***	***	***
	<i>SUS1</i>	***	***	*	*	**	***	n.s.
	<i>SPP1</i>	***	***	*	***	***	n.s.	n.s.

Note: Summary of the multivariate analysis is shown. * $P < 0.05$; ** $P < 0.01$; *** $P < 0.001$; n.s., not significant.

expression pattern, and expression patterns like ours have been documented in leaves of amaranth (*Amaranthus viridis*) (Nikolau and Klessig 1987), in peas (Sasaki et al. 1987) and beans (Bate et al. 1991) and rice (*Oryza sativa* L.) (Suzuki et al. 2001). Although the abundance of *rbcS* and *rbcL* is lower at 14 dpa than at the heading, the highest N concentrations in the pericarps occurred at 14 dpa. These observations suggest that Rubisco content and *rbcS* and *rbcL* abundance in wheat pericarps may not have a strong, positive correlation. This would be possible if wheat pericarps started to produce Rubisco at an increasing rate at heading and if Rubisco production continued between heading and 14 dpa, despite the decline in *rbcS* and *rbcL* expression. Alternatively, the degradation of Rubisco between heading and 14 dpa may

be minimal, in contrast to that in the flag leaves. The N concentrations of flag leaves across growth stages revealed that the highest Rubisco content may occur during leaf expansion as found by Suzuki et al. (2010). Therefore, our results suggest that there is an organ-specific variation in Rubisco biosynthesis/ degradation, N and C metabolism in wheat.

Carbon assimilation varied throughout ontogeny in a highly organ-specific manner

For most of the varieties, the highest *A* value was at 14 dpa both in wheat pericarps and flag leaves. Of the three genotypes, Huandoy showed the highest net spike photosynthesis (rate of photosynthesis × photosynthetic surface

Table 3. Heatmap of transcript abundance of *rbcL*, *rbcS*, *SPS1*, *SUS1* and *SPP1* genes related to photosynthesis and carbon metabolism in wheat pericarps and flag leaves at four growth stages.

Gene	Expression and fold change	Stage	Relative expression: pericarps			Relative expression: flag leaves			Fold change between organ types		
			Huandoy	Amurskaja	Greece	Huandoy	Amurskaja	Greece	Huandoy	Amurskaja	Greece
<i>rbcS</i>	Mean expression	Heading	5.00	13.94	14.97	31.06	26.53	45.87	6.21	1.90	3.06
		14-dpa	1.42	1.50	1.81	14.49	5.63	3.41	10.22	3.75	1.88
		30-dpa	0.74	0.45	2.29	4.56	4.77	2.28	6.16	10.57	1.00
	Fold change between growth stages	Heading and 14-dpa	3.53	9.29	8.27	2.14	4.72	13.45			
		Heading and 30-dpa	6.76	30.90	6.54	6.81	5.56	20.13			
		14-dpa and 30-dpa	1.92	3.33	0.79	3.18	1.18	1.50			
<i>rbcL</i>	Mean expression	Heading	414.81	519.31	303.81	1076.24	1009.80	873.87	2.59	1.94	2.88
		14-dpa	200.51	113.51	129.63	314.09	257.41	231.81	1.57	2.27	1.79
		30-dpa	94.47	64.63	130.06	124.54	147.86	125.65	1.32	2.29	0.97
	Fold change between growth stages	Heading and 14-dpa	2.07	4.58	2.34	3.43	3.92	3.77			
		Heading and 30-dpa	4.39	8.04	2.34	8.64	6.83	6.95			
		14-dpa and 30-dpa	2.12	1.76	1.00	2.52	1.74	1.84			
<i>SPS1</i>	Mean expression	Heading	0.64	1.31	1.23	3.68	6.13	5.51	5.80	4.67	4.49
		14-dpa	1.09	1.63	2.78	2.89	3.47	1.49	2.67	2.13	0.53
		30-dpa	1.42	0.47	1.41	8.90	3.06	1.92	6.28	6.47	1.36
	Fold change between growth stages	Heading and 14-dpa	0.59	0.81	0.44	1.27	1.77	3.71			
		Heading and 30-dpa	0.45	2.77	0.87	0.41	2.00	2.88			
		14-dpa and 30-dpa	0.77	3.44	1.98	0.33	1.13	0.78			
<i>SUS1</i>	Mean expression	Heading	1.27	2.65	4.23	4.47	3.31	4.81	3.51	1.25	1.14
		14-dpa	3.99	3.14	3.27	5.20	2.14	1.22	1.31	0.68	0.37
		30-dpa	2.93	1.57	2.02	8.36	4.96	5.13	2.85	3.16	2.53
	Fold change between growth stages	Heading and 14-dpa	0.32	0.84	1.29	0.86	1.55	3.95			
		Heading and 30-dpa	0.43	1.69	2.09	0.53	0.67	0.94			
		14-dpa and 30-dpa	1.36	2.00	1.62	0.62	0.43	0.24			
<i>SPP1</i>	Mean expression	Heading	0.79	1.49	4.05	0.97	1.25	2.39	1.24	0.84	0.59
		14-dpa	0.66	1.70	2.78	1.50	0.80	0.80	2.28	0.47	0.29
		30-dpa	0.72	1.38	2.70	1.03	1.17	1.53	1.42	0.85	0.57
	Fold change between growth stages	Heading and 14-dpa	1.19	0.88	1.46	0.65	1.57	2.99			
		Heading and 30-dpa	1.08	1.08	1.50	0.94	1.07	1.56			
		14-dpa and 30-dpa	0.91	1.23	1.03	1.46	0.68	0.52			

Note: Data presented are the mean values of gene expression. For relative expression, shades of red denote relatively higher expression, shades of yellow denote average expression, and shades of green denote relatively low expression. For fold changes, dark blue indicates greater fold changes, and light blue indicates moderate fold changes.

area of wheat spike) at all growth stages. Providing clues for the importance of spike photosynthesis for the grain filling and the harvest, Huandy showed the highest grain yield at maturity and highest spike weights at all growth stages. Further, spike weights of all the genotypes at all the growth stages were aligned with the net spike photosynthesis of each genotype.

After grain enlargement, the photosynthetic capacity of the flag leaves drastically declined while that of the spikes did not, so by 30 dpa there was no significant difference in V_{cmax} , J_{max} and TPU between these organs. This collapse in C assimilation by flag leaves coincided with leaf senescence. In both wheat spikes and flag leaves, the strong positive correlation of V_{cmax} and J_{max} accords with the results of Wullschleger (1993) based on analysis of $A-C_i$ curves for 109 plant species. The amount of Rubisco present in a photosynthetic organ decreases during senescence (Suzuki *et al.* 2001), and loss of Rubisco from flag leaves at late grain filling could explain the decreased rate of C assimilation at 30 dpa. This suggestion is supported by the observation in a following experiment that N concentration in flag leaves decreased in late grain filling compared to the heading and grain enlargement phases (Dehigaspitiya *et al.* 2019). Since

Rubisco constitutes 15–35% of the total N of a C_3 photosynthetic organ (Makino *et al.* 1992; Suzuki *et al.* 2009), lower N concentrations in flag leaves at late grain filling may indicate the presence of less Rubisco due to degradation. Furthermore, N concentrations of flag leaves were much higher than those of wheat pericarps around heading and 14 dpa, coincident with a greater expression of *rbcL* and *rbcS* mRNA. Moreover, the ratio of spike photosynthetic area and leaf photosynthetic area was lower at heading than during late grain filling. The preceding observations support the argument that flag leaves are the main driver of C assimilation during the heading and grain enlargement phase in wheat and that this role may be taken up by the spikes/pericarps during late grain filling.

Strong, positive correlations between spike dry weight and the product of biological capacity for C assimilation of wheat spikes and spike area were observed. Although the wheat leaves are the main driver of photosynthesis during heading and grain enlargement, C assimilation and sucrose metabolism of wheat spikes/pericarps is likely play an important role later during grain filling (Fig. S2). Therefore, the metabolic processes of wheat spikes/pericarps, such as

N metabolism and protein biosynthesis, and their contribution to grain quality under different environmental conditions merit further investigation.

In this study, biological capacity for C assimilation varied markedly between genotypes in both wheat spikes and flag leaves. Likewise, the biological capacity for C assimilation varied between plant growth stages. In general, the highest and the lowest $V_{c_{max}}$, J_{max} and TPU of wheat spikes occurred during grain enlargement and 30 dpa. Genetic variation in biochemical limitations to C assimilation in plants is known (Geber and Dawson 1997; Wullschlegel 1993), and is a governing factor for adaptive evolution in rates of C fixation (Geber and Dawson 1997). Other than genetic variation, plant development stage, organ type, plant nutrient supply and environmental conditions also influence the rate of C assimilation (Fan et al. 2011; Walker et al. 2014). Therefore, further research is required to elucidate the molecular mechanisms following the site specific, temporal and genotypic changes behind wheat grain filling for a higher yield.

Organ specific trends in the expression of key genes associated with sucrose metabolism

Sucrose is the main product of photosynthesis and plays important roles in growth, signal transduction, acclimation, growth and development in plants (Jia et al. 2015). Sucrose metabolism in higher plants is well characterised (Jia et al. 2015); however, to date, the site-specific and temporal variation of sucrose metabolism in wheat has not been intensely investigated. In general, the translocation of sucrose from its source to sink regulates the source and sink integration of the plant which in turn determines the plant growth and the yield (Bihmidine et al. 2013).

In this study, marked variation in transcript abundance of *SPS1*, *SUS1* and *SPP1* was found among organ types, indicating that sucrose metabolism varied in a site-specific manner. Further, growth stage and genotype also had a significant influence on the expression of the above genes. The correlation analysis between C assimilation in wheat spikes and mRNA abundance in wheat pericarps at heading showed strong, positive correlations between $V_{c_{max}}$ and *SPP1*, $V_{c_{max}}$ and *SUS1*, J_{max} and *SUS1*, and J_{max} and *SPP1*. Similarly, C assimilation and transcript abundance of *SPS1* and *SPP1* in pericarps had strong, positive correlations at 14 dpa.

A number of studies have suggested a correlation between photosynthesis and sucrose biosynthesis (Stitt 1986; Battistelli et al. 1991; Seneweera et al. 1995). SPS catalyses the biosynthesis of sucrose-6-phosphate from fructose-6-phosphate and UDP-glucose (Fig. S2). SPS has been identified as the main rate-limiting enzyme of sucrose synthesis (Seneweera et al. 1995; Lunn and MacRae 2003), and SPP is responsible for the final step of sucrose biosynthesis in plants. SPP catalyses the irreversible reaction of producing sucrose by hydrolysing sucrose-6-phosphate

(Jiang et al. 2015). In most plants, sucrose is the main transport carbohydrate, and it forms the interface between C assimilation and utilisation in source and sink tissues (Baxter et al. 2003). The amount of sucrose present in a photosynthetic organ depends on the rate of sucrose biosynthesis and the rate of sucrose export from the source (Ho and Thornley 1978; Baxter et al. 2003). The possibility of regulating the expression of genes associated with a number of metabolic pathways, including sucrose metabolism, has been reported (Koch et al. 1996; Baxter et al. 2003). According to our results, the highest photosynthetically active stage of wheat spikes was the heading and the grain enlargement phase. Interestingly, the highest expression of *SPS1* and *SPP1* was found at these growth stages (heading and 14 dpa) (Table 3). This suggests that sucrose metabolism in wheat pericarps may be regulated through a sugar sensing mechanism as reported by Koch et al. (1996) and Baxter et al. (2003). The higher expression of both *SPS1* and *SPP1* may reveal the increased sucrose synthesis in the wheat pericarp which then leads to higher C assimilation. Our results showed that biomass accumulation after heading mainly takes place in wheat spikes. Thus, the sucrose generated at wheat pericarps may be exported to the wheat endosperm. This suggestion is supported by the greatest biomass accumulation of wheat spikes commencing during the grain enlargement phase in all our wheat genotypes. Because of the strong interdependence of SPP and SPS, Echeverria et al. (1997) suggested that both SPP and SPS act together as a multienzyme complex in sucrose metabolism.

In a photosynthetic organ, sucrose is metabolised by either sucrose invertase to fructose and glucose or by SUS to UDP-glucose (Jiang et al. 2015). In general, higher SUS activity can be seen in source tissues. However, increased biomass production and/or sucrose content was reported in switchgrass (*Panicum virgatum*), tobacco (*Nicotiana tabacum* L.), cotton (*Gossypium hirsutum* L.) and poplar (*Panicum virgatum*) due to overexpression of SUS (Coleman et al. 2006; Coleman et al. 2009; Jiang et al. 2012; Poovaiah et al. 2015). Furthermore, phenotypic changes were exhibited in plants in which *SUS* was downregulated (Craig et al. 1999; Ruan et al. 2003). Consistent with this proposition, in the current study, the pericarps of the three wheat genotypes exhibited increased expression of *SUS1* during the grain enlargement phase; the phase which displayed the highest C assimilation and increase in biomass. This may also occur because during the grain enlargement phase, wheat grains exhibit more sink activities such as starch and amino acid biosynthesis. To facilitate these sink activities, sucrose cleavage has to be increased, and this is supported by the higher *SUS1* expression at grain enlargement phase in wheat pericarps. The products of sucrose cleavage in the wheat pericarp are then translocated to the wheat grain.

Data from this study as well as in other reported studies suggest that sucrose metabolism in wheat is influenced by the genotype, growth stage and organ type. Moreover, sucrose

metabolism in wheat pericarps may have a major role in wheat grain filling and, thereby, influence total yield. More research in this area is important to elucidate the complete mechanism of sucrose metabolism in wheat pericarps and understand its potential to increase crop yield.

Conclusions

The biological capacity for carbon assimilation in spikes and flag leaves of wheat are generally similar during late grain filling, although flag leaves displayed significantly higher rates from early to mid-grain filling. For the three genotypes, the net spike photosynthesis aligned with the spike weight at each growth stage. Transcript abundance of *rbcS* and *rbcL*, N contents and C assimilation in wheat pericarps and flag leaves revealed that pericarps and flag leaves act differently during Rubisco biosynthesis. Finally, the expression of key genes associated with sucrose metabolism revealed genotypic, site-specific and temporal influences on sucrose metabolism in wheat and the influence of the metabolites of sucrose metabolism on gene expression. Interestingly, transcript abundance during sucrose metabolism and photosynthesis in wheat pericarps confirms that metabolic processes of spikes may have a significant role in grain filling and, hence on total yield. However, further research is required to elucidate the site-specific changes in the key metabolic processes such as protein biosynthesis, source and sink balance, photosynthesis, sucrose metabolism and N assimilation along with their interactions to get a holistic understanding of grain filling and, thereby, provide new avenues to improve the yield of future crops.

Supplementary material

Supplementary material is available [online](#).

References

- Bachir DG, Saeed I, Song Q, Linn TZ, Chen L, Hu Y-G (2017) Characterization and expression patterns of key C₄ photosynthetic pathway genes in bread wheat (*Triticum aestivum* L.) under field conditions. *Journal of Plant Physiology* **213**, 87–97. doi:10.1016/j.jplph.2017.03.002
- Barbottin A, Lecomte C, Bouchard C, Jeuffroy M-H (2005) Nitrogen remobilization during grain filling in wheat: genotypic and environmental effects. *Crop Science* **45**, 1141–1150. doi:10.2135/cropsci2003.0361
- Bate NJ, Rothstein SJ, Thompson JE (1991) Expression of nuclear and chloroplast photosynthesis-specific genes during leaf senescence. *Journal of Experimental Botany* **42**, 801–811. doi:10.1093/jxb/42.6.801
- Battistelli A, Adcock MD, Leegood RC (1991) The relationship between the activation state of sucrose-phosphate synthase and the rate of CO₂ assimilation in spinach leaves. *Planta* **183**, 620–622. doi:10.1007/BF00194285
- Baxter CJ, Foyer CH, Turner J, Rolfe SA, Quick WP (2003) Elevated sucrose-phosphate synthase activity in transgenic tobacco sustains photosynthesis in older leaves and alters development. *Journal of Experimental Botany* **54**, 1813–1820. doi:10.1093/jxb/erg196
- Bihmidine S, Hunter III CT, Johns CE, Koch KE, Braun DM (2013) Regulation of assimilate import into sink organs: update on molecular drivers of sink strength. *Frontiers in Plant Science* **4**, 177. doi:10.3389/fpls.2013.00177
- Coleman HD, Ellis DD, Gilbert M, Mansfield SD (2006) Up-regulation of sucrose synthase and UDP-glucose pyrophosphorylase impacts plant growth and metabolism. *Plant Biotechnology Journal* **4**, 87–101. doi:10.1111/j.1467-7652.2005.00160.x
- Coleman HD, Yan J, Mansfield SD (2009) Sucrose synthase affects carbon partitioning to increase cellulose production and altered cell wall ultrastructure. *Proceedings of the National Academy of Sciences* **106**, 13118–13123. doi:10.1073/pnas.0900188106
- Craig J, Barratt P, Tatge H, Déjardin A, Handley L, Gardner CD, Barber L, Wang T, Hedley C, Martin C (1999) Mutations at the *rug4* locus alter the carbon and nitrogen metabolism of pea plants through an effect on sucrose synthase. *The Plant Journal* **17**, 353–362. doi:10.1046/j.1365-313X.1999.00382.x
- Darroch BA, Baker RJ (1990) Grain filling in three spring wheat genotypes: statistical analysis. *Crop Science* **30**, 525–529. doi:10.2135/cropsci1990.0011183X003000030009x
- Dean C, Pichersky E, Dunsmuir P (1989) Structure, evolution, and regulation of *RbcS* genes in higher plants. *Annual Review of Plant Physiology and Plant Molecular Biology* **40**, 415–439. doi:10.1146/annurev.pp.40.060189.002215
- Dehigaspitiya P, Milham P, Ash GJ, Arun-Chinnappa K, Gamage D, Martin A, Nagasaka S, Seneweera S (2019) Exploring natural variation of photosynthesis in a site-specific manner: evolution, progress, and prospects. *Planta* **250**, 1033–1050. doi:10.1007/s00425-019-03223-1
- Demirevska K, Zasheva D, Dimitrov R, Simova-Stoilova L, Stamenova M, Feller U (2009) Drought stress effects on Rubisco in wheat: changes in the Rubisco large subunit. *Acta Physiologiae Plantarum* **31**, 1129–1138. doi:10.1007/s11738-009-0331-2
- Dillard HR (2019) Global food and nutrition security: from challenges to solutions. *Food Security* **11**, 249–252. doi:10.1007/s12571-019-00893-3
- Echeverria E, Salvucci ME, Gonzalez P, Paris G, Salerno G (1997) Physical and kinetic evidence for an association between sucrose-phosphate synthase and sucrose-phosphate phosphatase. *Plant Physiology* **115**, 223–227. doi:10.1104/pp.115.1.223
- Evans JR, Santiago LS (2014) PrometheusWiki Gold Leaf Protocol: gas exchange using LI-COR 6400. *Functional Plant Biology* **41**, 223–226. doi:10.1071/FP10900
- Fan Y, Zhong Z, Zhang X (2011) Determination of photosynthetic parameters V_{cmax} and J_{max} for a C₃ plant (spring hulless barley) at two altitudes on the Tibetan Plateau. *Agricultural and Forest Meteorology* **151**, 1481–1487. doi:10.1016/j.agrformet.2011.06.004
- Furbank RT, Quick WP, Sirault XRR (2015) Improving photosynthesis and yield potential in cereal crops by targeted genetic manipulation: prospects, progress and challenges. *Field Crops Research* **182**, 19–29. doi:10.1016/j.fcr.2015.04.009
- Geber MA, Dawson TE (1997) Genetic variation in stomatal and biochemical limitations to photosynthesis in the annual plant, *Polygonum arenastrum*. *Oecologia* **109**, 535–546. doi:10.1007/s004420050114
- Ho LC, Thornley JHM (1978) Energy requirements for assimilate translocation from mature tomato leaves. *Annals of Botany* **42**, 481–483. doi:10.1093/oxfordjournals.aob.a085484
- Jenner CF, Ugalde TD, Aspinall D (1991) The physiology of starch and protein deposition in the endosperm of wheat. *Functional Plant Biology* **18**, 211–226. doi:10.1071/PP9910211
- Jia S, Lv J, Jiang S, Liang T, Liu C, Jing Z (2015) Response of wheat ear photosynthesis and photosynthate carbon distribution to water deficit. *Photosynthetica* **53**, 95–109. doi:10.1007/s11099-015-0087-4
- Jiang S-Y, Chi Y-H, Wang J-Z, Zhou J-X, Cheng Y-S, Zhang B-L, Ma A, Vanitha J, Ramachandran S (2015) Sucrose metabolism gene families and their biological functions. *Scientific Reports* **5**, 17583. doi:10.1038/srep17583
- Jiang Y, Guo W, Zhu H, Ruan Y-L, Zhang T (2012) Overexpression of GhSusA1 increases plant biomass and improves cotton fiber yield and quality. *Plant Biotechnology Journal* **10**, 301–312. doi:10.1111/j.1467-7652.2011.00662.x

- Koch K (2004) Sucrose metabolism: regulatory mechanisms and pivotal roles in sugar sensing and plant development. *Current Opinion in Plant Biology* **7**, 235–246. doi:10.1016/j.pbi.2004.03.014
- Koch KE, Wu Y, Xu J (1996) Sugar and metabolic regulation of genes for sucrose metabolism: potential influence of maize sucrose synthase and soluble invertase responses on carbon partitioning and sugar sensing. *Journal of Experimental Botany* **1179**–1185. doi:10.1093/jxb/47.Special_Issue.1179
- Kubis A, Bar-Even A (2019) Synthetic biology approaches for improving photosynthesis. *Journal of Experimental Botany* **70**(5), 1425–1433. doi:10.1093/jxb/erz029
- Li Y, Heckmann D, Lercher MJ, Maurino VG (2017) Combining genetic and evolutionary engineering to establish C₄ metabolism in C₃ plants. *Journal of Experimental Botany* **68**, 117–125. doi:10.1093/jxb/erw333
- Lunn JE, MacRae E (2003) New complexities in the synthesis of sucrose. *Current Opinion in Plant Biology* **6**, 208–214. doi:10.1016/S1369-5266(03)00033-5
- Makino A, Mae T, Ohira K (1984) Relation between nitrogen and ribulose-1,5-bisphosphate carboxylase in rice leaves from emergence through senescence. *Plant and Cell Physiology* **25**, 429–437. doi:10.1093/oxfordjournals.pcp.a076730
- Makino A, Sakashita H, Hidema J, Mae T, Ojima K, Osmond B (1992) Distinctive responses of ribulose-1,5-bisphosphate carboxylase and carbonic anhydrase in wheat leaves to nitrogen nutrition and their possible relationships to CO₂-transfer resistance. *Plant Physiology* **100**, 1737–1743. doi:10.1104/pp.100.4.1737
- Molero G, Reynolds MP (2020) Spike photosynthesis measured at high throughput indicates genetic variation independent of flag leaf photosynthesis. *Field Crops Research* **255**, 107866. doi:10.1016/j.fcr.2020.107866
- Nie G, Hendrix DL, Webber AN, Kimball BA, Long SP (1995) Increased accumulation of carbohydrates and decreased photosynthetic gene transcript levels in wheat grown at an elevated CO₂ concentration in the field. *Plant Physiology* **108**, 975–983. doi:10.1104/pp.108.3.975
- Nikolau BJ, Klessig DF (1987) Coordinate, organ-specific and developmental regulation of ribulose 1,5-bisphosphate carboxylase gene expression in *Amaranthus hypochondriacus*. *Plant Physiology* **85**, 167–173. doi:10.1104/pp.85.1.167
- Paul MJ, Pellny TK (2003) Carbon metabolite feedback regulation of leaf photosynthesis and development. *Journal of Experimental Botany* **54**, 539–547. doi:10.1093/jxb/erg052
- Poovaliah CR, Mazarei M, Decker SR, Turner GB, Sykes RW, Davis MF, Stewart CN (2015) Transgenic switchgrass (*Panicum virgatum* L.) biomass is increased by overexpression of switchgrass sucrose synthase (*PvSUS1*). *Biotechnology Journal* **10**, 552–563. doi:10.1002/biot.201400499
- Rajala A, Hakala K, Mäkelä P, Muurinen S, Peltonen-Sainio P (2009) Spring wheat response to timing of water deficit through sink and grain filling capacity. *Field Crops Research* **114**, 263–271. doi:10.1016/j.fcr.2009.08.007
- Rangan P, Furtado A, Henry RJ (2016) New evidence for grain specific C₄ photosynthesis in wheat. *Scientific Reports* **6**, 31721. doi:10.1038/srep31721
- Ruan Y-L, Llewellyn DJ, Furbank RT (2003) Suppression of sucrose synthase gene expression represses cotton fiber cell initiation, elongation, and seed development. *The Plant Cell* **15**, 952–964. doi:10.1105/tpc.010108
- Sasaki Y, Nakamura Y, Matsuno R (1987) Regulation of gene expression of ribulose bisphosphate carboxylase in greening pea leaves. *Plant Molecular Biology* **8**, 375–382. doi:10.1007/BF00015815
- Seneweera S, Makino A, Hirotsu N, Norton R, Suzuki YJE, Botany E (2011) New insight into photosynthetic acclimation to elevated CO₂: the role of leaf nitrogen and ribulose-1,5-bisphosphate carboxylase/oxygenase content in rice leaves. *Environmental and Experimental Botany* **71**, 128–136. doi:10.1016/J.ENVEXPBOT.2010.11.002
- Seneweera SP, Basra AS, Barlow EW, Conroy JP (1995) Diurnal regulation of leaf blade elongation in rice by CO₂: Is it related to sucrose-phosphate synthase activity? *Plant Physiology* **108**, 1471–1477. doi:10.1104/pp.108.4.1471
- Serrago RA, Alzueta I, Savin R, Slafer GA (2013) Understanding grain yield responses to source–sink ratios during grain filling in wheat and barley under contrasting environments. *Field Crops Research* **150**, 42–51. doi:10.1016/j.fcr.2013.05.016
- Stitt M (1986) Limitation of photosynthesis by carbon metabolism: I. Evidence for excess electron transport capacity in leaves carrying out photosynthesis in saturating light and CO₂. *Plant Physiology* **81**, 1115–1122. doi:10.1104/pp.81.4.1115
- Stitt M, Lunn J, Usadel B (2010) Arabidopsis and primary photosynthetic metabolism – more than the icing on the cake. *The Plant Journal* **61**, 1067–1091. doi:10.1111/j.1365-3113X.2010.04142.x
- Suzuki Y, Kihara-Doi T, Kawazu T, Miyake C, Makino A (2010) Differences in Rubisco content and its synthesis in leaves at different positions in Eucalyptus globulus seedlings. *Plant, Cell & Environment* **33**, 1314–1323. doi:10.1111/j.1365-3040.2010.02149.x
- Suzuki Y, Makino A, Mae T (2001) Changes in the turnover of Rubisco and levels of mRNAs of *rbcL* and *rbcS* in rice leaves from emergence to senescence. *Plant, Cell & Environment* **24**, 1353–1360. doi:10.1046/j.0016-8025.2001.00789.x
- Suzuki Y, Miyamoto T, Yoshizawa R, Mae T, Makino A (2009) Rubisco content and photosynthesis of leaves at different positions in transgenic rice with an overexpression of *RBCS*. *Plant, Cell & Environment* **32**, 417–427. doi:10.1111/j.1365-3040.2009.01937.x
- van Bezouw RFHM, Keurentjes JJB, Harbinson J, Aarts MGM (2019) Converging phenomics and genomics to study natural variation in plant photosynthetic efficiency. *The Plant Journal* **97**, 112–133. doi:10.1111/tbj.14190
- Vicente R, Pérez P, Martínez-Carrasco R, Usadel B, Kostadinova S, Morcuende R (2015) Quantitative RT–PCR platform to measure transcript levels of C and N metabolism-related genes in durum wheat: transcript profiles in elevated [CO₂] and high temperature at different levels of N supply. *Plant and Cell Physiology* **56**, 1556–1573. doi:10.1093/pcp/pcv079
- Vu JC, Allen Jr. LH, Gesch RW (2006) Up-regulation of photosynthesis and sucrose metabolism enzymes in young expanding leaves of sugarcane under elevated growth CO₂. *Plant Science* **171**, 123–131. doi:10.1016/j.plantsci.2006.03.003
- Walker AP, Beckerman AP, Gu L, Kattge J, Cernusak LA, Domingues TF, Scales JC, Wohlfahrt G, Wullschlegel SD, Woodward FI (2014) The relationship of leaf photosynthetic traits – V_{c,max} and J_{max} – to leaf nitrogen, leaf phosphorus, and specific leaf area: a meta-analysis and modeling study. *Ecology and Evolution* **4**, 3218–3235. doi:10.1002/ece3.1173
- Wang S, Tholen D, Zhu X-G (2017) C₄ photosynthesis in C₃ rice: a theoretical analysis of biochemical and anatomical factors. *Plant, Cell & Environment* **40**, 80–94. doi:10.1111/pce.12834
- White JC, Gardea-Torresdey J (2018) Achieving food security through the very small. *Nature Nanotechnology* **13**, 627. doi:10.1038/s41565-018-0223-y
- Wullschlegel SD (1993) Biochemical limitations to carbon assimilation in C₃ plants—a retrospective analysis of the A/C_i curves from 109 species. *Journal of Experimental Botany* **44**, 907–920. doi:10.1093/jxb/44.5.907
- Zhang M, Gao Y, Zhang Y, Fischer T, Zhao Z, Zhou X, Wang Z, Wang E (2020) The contribution of spike photosynthesis to wheat yield needs to be considered in process-based crop models. *Field Crops Research* **257**, 107931. doi:10.1016/j.fcr.2020.107931

Data availability. The data that support this study are available in the article and accompanying online supplementary material.

Conflicts of interest. The authors declare no conflicts of interest.

Declaration of funding. This study was funded by the University of Southern Queensland, Australia.

Acknowledgements. Prabuddha was supported by the University of Southern Queensland to conduct his Ph.D. by providing him with a higher degree research scholarship.

Author affiliations

^ACentre for Crop Health, University of Southern Queensland, Toowoomba, Qld 4350, Australia.

^BHawkesbury Institute for the Environment, Western Sydney University, LB 1797, Penrith, NSW 2753, Australia.

^CDepartment of Agricultural Biology, Faculty of Agriculture, University of Ruhuna, Matara, Sri Lanka.

^DSchool of Science, Western Sydney University, LB 1797, Penrith, NSW 2753, Australia.

^EFaculty of Veterinary and Agriculture Science, University of Melbourne, Parkville, Vic. 3010, Australia.